

High temperature electrochemical behaviors of ramsdellite $\text{Li}_2\text{Ti}_3\text{O}_7$ and its Fe-doped derivatives for lithium ion batteries

Shuhua Ma^{*}, Hideyuki Noguchi

Department of Applied Chemistry, Saga University, Saga 840-0852, Japan

Received 16 January 2006; received in revised form 2 June 2006; accepted 7 June 2006

Available online 25 July 2006

Abstract

The high temperature electrochemical cell performances of $\text{Li}_2\text{Ti}_3\text{O}_7$ and its Fe-doped derivatives were studied. Pure $\text{Li}_2\text{Ti}_3\text{O}_7$ gave higher charge/discharge capacities at 40 and 50 °C than at room temperature and featured good cycleabilities among the initial 40 cycles. However, the cell performance was terribly deteriorated at 70 °C. XRD measurement revealed its structure degradation into a rocksalt-type cubic structure phase with lower crystallinity in this high temperature of 70 °C. The XRD results from the electrodes experienced different cycles at 40 °C showed that the structure degradation is gradually developed as the cell is cycled. Meanwhile, Fe-doped $\text{Li}_2\text{Ti}_3\text{O}_7$ ramsdellite samples afforded improved insertion/extraction properties of the lithium ions, even at 70 °C. The improved high temperature performance is presumed considered from the stabilization of the foreign iron metal ions for ramsdellite structure.

© 2006 Elsevier B.V. All rights reserved.

Keywords: Lithium battery; Anode material; Ramsdellite; Fe-doped $\text{Li}_2\text{Ti}_3\text{O}_7$; High temperature; Performance deterioration

1. Introduction

Lithium titanate oxides exist various polymorphs, for example, rutile ($P4_2/mnm$), anatase ($I4_1/amd$), brookite ($Pbca$), ramsdellite ($Pnma$), colombite ($Pcbn$), spinel ($Fd3m$), and orthorhombic one ($Imma$) [1]. At present, the investigations as anode materials are mainly concentrated on spinel, $\text{Li}_4\text{Ti}_5\text{O}_{12}$, ramsdellite, $\text{Li}_2\text{Ti}_3\text{O}_7$, and their related solid solutions due to their lower voltage [2–12]. Research works for electrochemical cell performance of $\text{Li}_2\text{Ti}_3\text{O}_7$ have been carried out at room temperature with focus on the preparation, structure characterization and electrochemical cell performance, and it was believed that this host structure is stable during charge/discharge cycles at usual environmental temperatures [3–5,10,11]. Applications exposed to the temperatures of higher than 50 °C are common in tropical area, especially for appliances with poor ventilation cooling like electric vehicle. Therefore, high temperature

behavior of electrode materials for lithium ion batteries is a crucial assessment specification, which sometimes could suspended their use, e.g., pure LiMn_2O_4 spinel, in spite of the prominences in cost, environment allowance, and cell performance at room temperature [13].

In this preliminary work, the high temperature electrochemical cell performances of $\text{Li}_2\text{Ti}_3\text{O}_7$ and Fe-doped $\text{Li}_2\text{Ti}_3\text{O}_7$ were studied in view of their potential utility as anode materials for lithium batteries. $\text{Li}_2\text{Ti}_3\text{O}_7$ exhibited excellent cycling performance and a gradually enhanced discharge capacity as the operating temperature increased between RT and 50 °C. However, a structure degradation was strengthened as cycled at 70 °C, which triggered a rapid deterioration in cell performance at this significantly elevated cycling temperature.

Meanwhile, cycling and capacity performances at 70 °C were significantly improved with doping Fe impurity into $\text{Li}_2\text{Ti}_3\text{O}_7$ ramsdellite structure by firing at a much decreased preparing temperature. XRD measurement did not detect any structure collapse for the Fe-doped ramsdellite as cycled at the same high temperature as that for the pure $\text{Li}_2\text{Ti}_3\text{O}_7$ ramsdellite. The improved high temperature performance is presumed considered from the stabilization of the foreign metal, Fe, in ramsdellite framework structure.

^{*} Corresponding author at: Technical Development Headquarters, ESPEC Corp., 5-2-5, Minamimachi, Kanokodai, Kita-ku, Kobe, Hyogo 651-1515, Japan. Tel.: +81 78 951 0972; fax: +81 78 951 0976.

E-mail address: s-ma@espec.co.jp (S. Ma).

2. Experimental

The chemically stoichiometric mixture of source materials, titanium dioxide (anatase), $\text{CH}_3\text{COOLi}\cdot 2\text{H}_2\text{O}$, or/and FeOOH , was ground thoroughly and then preheated at 750°C for 5 h. After cooling and grinding, it was pressed into a pellet and then calcined again at an appointed temperature for 20 h, that are 1050 and 950°C for pure $\text{Li}_2\text{Ti}_3\text{O}_7$ and Fe-doped ramsdellites, respectively. After pulverized and ground, the sample was kept in store for use.

The phase identification and structure detection were carried out by X-ray diffraction using Rigaku RINT1000 X-ray diffractometer (Rigaku Ltd., Japan) with $\text{Cu K}\alpha$ (1.5414 \AA) radiation, which was monochromized by a graphite crystal.

Charge/discharge test was carried out in a CR2032 coin-type cell, which consisted of a cathode and an excess amount of metallic lithium anode separated by a Celgard 2400 porous polypropylene film. The cathode film with 30 mg of electrode material and 10 mg of TAB-2 (teflonized acetylene black) as conducting binder was pressed onto a stainless steel screen disk (16 mm in diameters) at 6 tonnes, and fabricated into the cell as the cathode after dried at 200°C for 4 h. The electrolyte used was 1 M LiPF_6 EC (ethylene carbonate)/DMC (dimethyl carbonate) 1:2 by volume. Cells were cycled at a current rate of 0.4 mA cm^{-2} (C/6).

The high temperature discharge/charge measurements were carried out in a self-made hot box with oscillation range of $\pm 2^\circ\text{C}$.

3. Results and discussion

3.1. Dependence of cell performance of $\text{Li}_2\text{Ti}_3\text{O}_7$ ramsdellite on operating temperature

3.1.1. Cell performance at room and elevated temperatures

Fig. 1 shows discharge/charge curves of the initial one and half cycles at room temperature (RT), 40°C , 50°C , and 70°C for ramsdellite $\text{Li}_2\text{Ti}_3\text{O}_7$ sample prepared at 1050°C . All the discharge/charge curves characterize typical $\text{Li}_2\text{Ti}_3\text{O}_7$ ramsdellite pattern in initial cycles at the various operating temperatures. In RT, the whole discharge/charge curves consist of three inclined parts with different gradient, situated in voltage ranges of between 2.1 and 1.8, 1.8 and 1.5, and 1.5 and 1.2 V, respectively. Arroyo y de Dompablo et al. have attributed them into two consecutive solid solutions and a biphasic region [5,10]. Further, with the increase in operating temperature, the cycling capacity was increased. As shown in Fig. 1, the discharge curves of sample operated at various temperatures, except 70°C , resemble each other, with an improved capacity as the increase in temperature. In view of its temperature dependence, it can be tentatively considered that the activation of some inert sites, which are potentially available for the insertion/extraction of lithium ions at RT, by the elevated operating temperatures may be responsible for this capacity enhancement. The results show that a typical lithium ion intercalation/deintercalation process in $\text{Li}_2\text{Ti}_3\text{O}_7$ ramsdellite structure has occurred at all the above temperature environments.

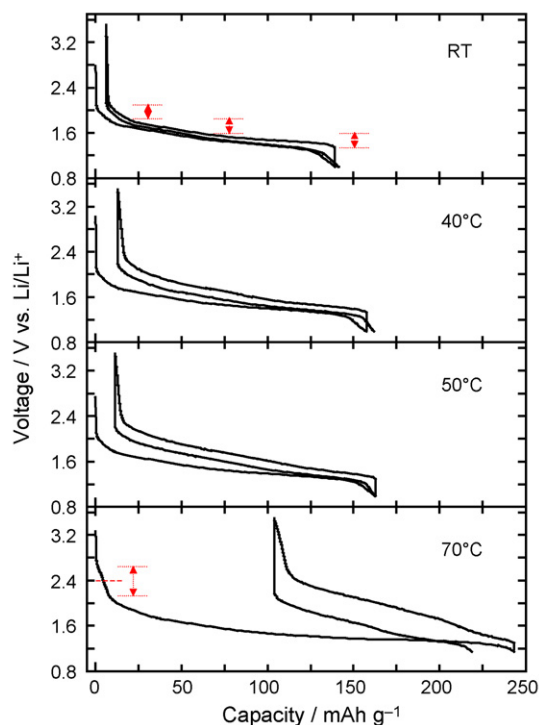


Fig. 1. Discharge/charge curves in initial first and half cycles of $\text{Li}_2\text{Ti}_3\text{O}_7$ electrode at various operating temperatures in electrolyte of 1 M LiPF_6 EC/DMC 1:2 (in volume). Galvanostatic current density: 0.4 mA cm^{-2} ; voltage range: 1.0–3.5 V for RT, 40 and 50°C and 1.15–3.5 V for 70°C .

On the other hand, the increase in charge capacity is relatively a little smaller than that in discharge capacity, which leads to the irreversible capacity, i.e., the difference between the discharge and charge capacities. It can be observed that increases in irreversible capacity were incurred with the increases of operation temperature from RT to 70°C . Here, it must be mentioned that, in this paper, the terms of charge and discharge signified increased and decreased voltage-changing processes, respectively, which is following the normal practice for the cathode or the whole battery instead of that for the anode regime. For example, the discharge capacity operated at 70°C increased rapidly up to ca. 245 mAh g^{-1} , however, the charge capacity is only 120 mAh g^{-1} . Considering that the reductive decomposition of solvents in electrolyte occurs at ca. 1.0 V versus Li^+/Li [14], the cut-off voltage has been determined to be 1.15 V versus Li^+/Li for 70°C . Even so, a big irreversible capacity loss has also been observed here. Further, it was noted that an additional narrow plateau area has been developed with the elevated temperature around about 2.4 V versus Li^+/Li at 70°C . Therefore, the high irreversible capacity in the operation at 70°C was considered to come mainly from the decomposition of $\text{Li}_2\text{Ti}_3\text{O}_7$ material into some products between 2.6 and 1.15 V versus Li^+/Li , instead of the electrochemical reduction of the solvents in the electrolyte. The results indicated that a deterioration process has occurred in this voltage range with the elevated operating temperatures, especially at 70°C .

Herein, an interesting fact can also be recognized from Fig. 1. Excellent lithium ions insertion/extraction properties were delivered at between RT and 50°C , however, an identifiable

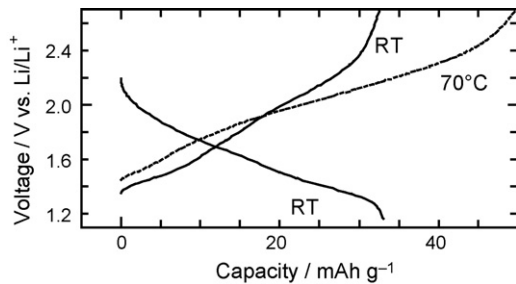


Fig. 2. The 25th charge curve at 70 °C and the followed discharge/charge curves after moved from hot box and cooled to RT for $\text{Li}_2\text{Ti}_3\text{O}_7$ electrode in electrolyte of 1 M LiPF_6 EC/DMC 1:2 (in volume). Galvanostatic current density: 0.4 mA cm^{-2} ; voltage range: 1.0–3.5 V for RT and 1.15–3.5 V for 70 °C.

enlarged charge/discharge polarization, the scope of difference between charge and discharge potentials, can still be found as the increase in operating temperature. This phenomenon is strange because the diffusion rate of Li would be increased at the elevated temperatures. Moreover, the cell performance was terribly deteriorated at 70 °C after the first discharge. The first charge capacity is 120 mAh g^{-1} , which is smaller than those at 40 and 50 °C. When the charged cell was cooled from 70 °C to RT after 25 cycles, the charge capacity has decreased from 50 to 32 mAh g^{-1} as shown in Fig. 2. The discharge voltage of the cooled cell also decreased rapidly, which is completely different from that operated only at RT. The results suggest that an irreversible structural transformation of $\text{Li}_2\text{Ti}_3\text{O}_7$ phase may have occurred upon exposing the cell to high temperature cycling.

The above facts can be observed more clearly from the cycling performances of ramsdellite $\text{Li}_2\text{Ti}_3\text{O}_7$ sample at various operating temperatures as shown in Fig. 3. The cell still gave a good discharge capacity retention at 50 °C up to the 30th cycles, which is comparable to that at RT; whereas, a successive capacity fading can be observed at 70 °C.

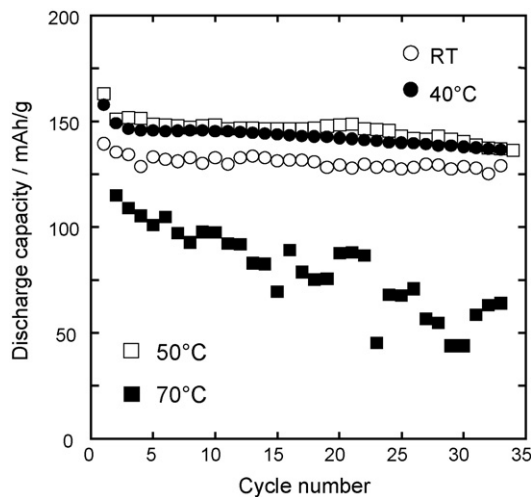


Fig. 3. Variation of specific discharge capacity with cycle number for $\text{Li}_2\text{Ti}_3\text{O}_7$ electrode at various operating temperatures in electrolyte of 1 M LiPF_6 EC/DMC 1:2 (in volume). Galvanostatic current density: 0.4 mA cm^{-2} ; voltage range: 1.0–3.5 V for RT, 40 and 50 °C and 1.15–3.5 V for 70 °C.

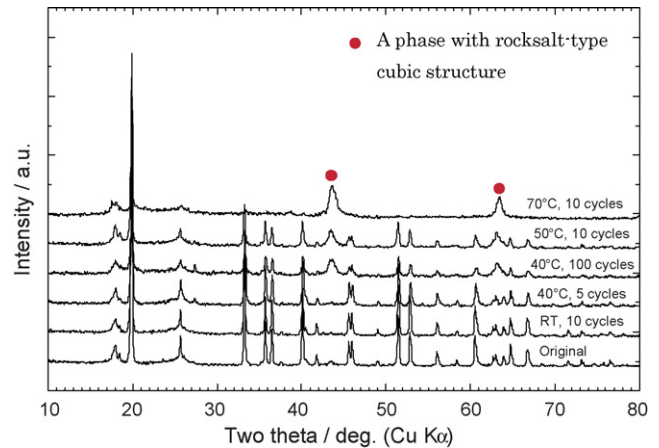


Fig. 4. Powder X-ray diffraction patterns of $\text{Li}_2\text{Ti}_3\text{O}_7$ electrode before and after cycled a certain times at various operating temperatures.

3.1.2. Deterioration in cell performance at 70 °C

In order to ascertain what have happened in this high operating temperature of 70 °C, XRD patterns of fully charged electrodes experienced different cycles at various operating temperatures are shown in Fig. 4. It can be found that there occurred two new peaks for 70 °C, which may indicate a kind of rocksalt-type cubic structure, at 43.6° and 63.6° in high 2θ degree area with the disappearance of original peaks of $\text{Li}_2\text{Ti}_3\text{O}_7$ phase. The result suggests that the ramsdellite structure was remarkably destroyed and almost degraded into a rocksalt-type cubic structure phase with much lower crystallinity in 70 °C only after 10 cycles; whereas, the ramsdellite structure was maintained in 50 °C after the same cycles, although the two peaks from the rocksalt-type cubic structure phase at 43.6° and 63.6° of 2θ can also be detected. The result indicates that a structure collapse has been developed as the increase in operating temperature, which related with the deterioration in the first discharge and the followed cycling operation observed at the elevated temperatures, especially, 70 °C.

We also studied effect of cycling experience on electrode structure at 40 °C. It can be found, also from Fig. 4, that the structure degradation into a rocksalt-type cubic structure phase has occurred after a long discharge/charge cycling of 100 cycles, though no obvious structure changes can be detected in the first 5 cycles. The result demonstrated that the structure degradation was gradually developed as the cell cycled at elevated operating temperatures. However, the operating temperatures above 70 °C greatly accelerated this structure collapse.

3.2. High temperature discharge/charge performance of Fe-doped $\text{Li}_2\text{Ti}_3\text{O}_7$ ramsdellite

Fe can be doped into $\text{Li}_2\text{Ti}_3\text{O}_7$ ramsdellite structure and form a $\text{Li}_2\text{O}-\text{Fe}_2\text{O}_3-\text{TiO}_2$ -based ramsdellite solid solution [15]. Fe-doped $\text{Li}_2\text{Ti}_3\text{O}_7$ ramsdellites, $\text{Li}_{1.73}[\text{Li}_{0.48}\text{Fe}_{0.30}\text{Ti}_{3.22}]\text{O}_8$ and $\text{Li}_{1.78}[\text{Li}_{0.38}\text{Fe}_{0.63}\text{Ti}_{2.99}]\text{O}_8$, prepared at 950 °C were examined to study the effect of Fe substitution on high temperature cell properties of $\text{Li}_2\text{Ti}_3\text{O}_7$ ramsdellite. Fig. 5 shows the first and half discharge/charge curves of $\text{Li}_{1.73}[\text{Li}_{0.48}\text{Fe}_{0.30}\text{Ti}_{3.22}]\text{O}_8$

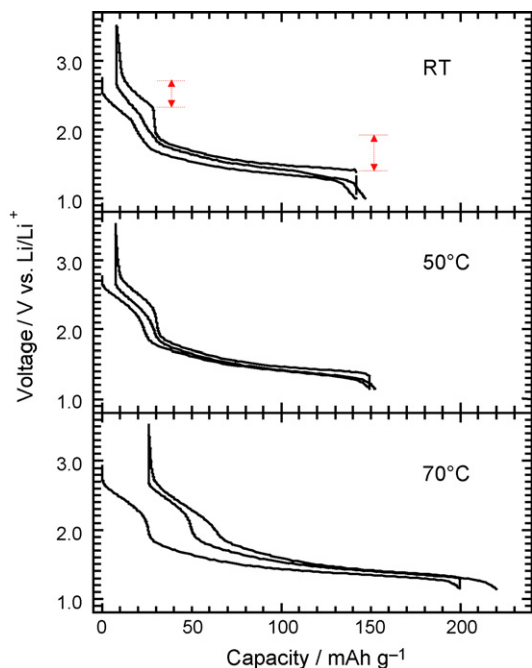


Fig. 5. Discharge/charge curves in initial first and half cycles of $\text{Li}_{1.73}[\text{Li}_{0.48}\text{Fe}_{0.30}\text{Ti}_{3.22}]\text{O}_8$ electrode at RT, 50 and 70 °C in electrolyte of 1 M LiPF_6 EC/DMC 1:2 (in volume). Galvanostatic current density: 0.4 mA cm^{-2} ; voltage range: 1.0–3.5 V for RT and 50 °C and 1.2–3.5 V for 70 °C.

electrode at RT, 50 and 70 °C, respectively. It can be found that there exist two plateaus, situated between 2.7 and 2.3 and 1.9 and 1.3 V versus Li^+/Li , which can be attributed to the reduction/oxidation of $\text{Fe}^{3+}/\text{Fe}^{2+}$ and $\text{Ti}^{4+}/\text{Ti}^{3+}$ couples, respectively. Furthermore, no enlarged charge/discharge voltage polarization can be found at 50 and 70 °C. It also can be observed that the discharge/charge capacity increased with the increase in operating temperature, which has been tentatively attributed to the activation of some inert sites as before. The cycleability at 70 °C has been improved by Fe-doping to $\text{Li}_2\text{Ti}_3\text{O}_7$ as shown in Fig. 6.

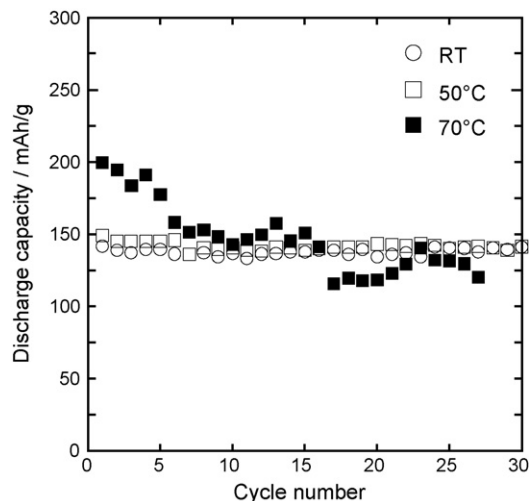


Fig. 6. Cycling performance of $\text{Li}_{1.73}[\text{Li}_{0.48}\text{Fe}_{0.30}\text{Ti}_{3.22}]\text{O}_8$ sample at RT, 50 and 70 °C in electrolyte of 1 M LiPF_6 EC/DMC 1:2 (in volume). Galvanostatic current density: 0.4 mA cm^{-2} ; voltage range: 1.0–3.5 V for RT and 50 °C and 1.2–3.5 V for 70 °C.

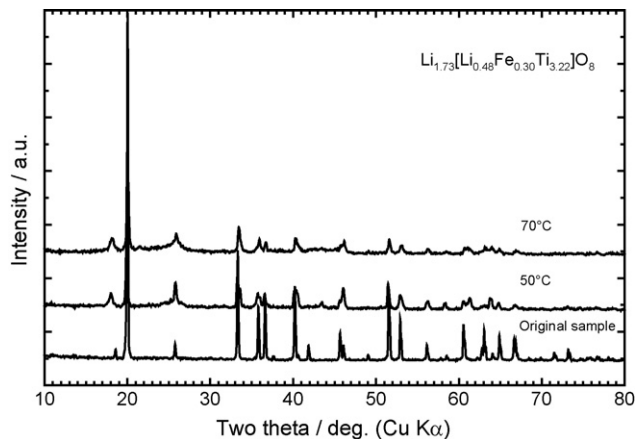


Fig. 7. Powder X-ray diffraction patterns of $\text{Li}_{1.73}[\text{Li}_{0.48}\text{Fe}_{0.30}\text{Ti}_{3.22}]\text{O}_8$ sample and electrodes after five cycles at 50 and 70 °C.

Although the capacity at 70 °C has been decreased to around 150 mAh g^{-1} after five cycles, an acceptable cycling performance is available thereafter. XRD patterns of charged electrode were measured for various operating temperatures in order to explore the origin of the improved cell performance at 70 °C. XRD profiles of electrodes after five cycles kept initial original profiles, though peaks became a little wider at 70 °C as shown in Fig. 7. It can be found that the retention of the ramsdellite structure was attained by means of the substitution of Fe into $\text{Li}_2\text{Ti}_3\text{O}_7$ ramsdellite, even exposed to high temperature cycling at 70 °C.

The electrochemical behavior of the Fe-doped ramsdellite with higher Fe doping content, $\text{Li}_{1.78}[\text{Li}_{0.38}\text{Fe}_{0.63}\text{Ti}_{2.99}]\text{O}_8$, has also been studied. The discharge/charge profiles are shown in

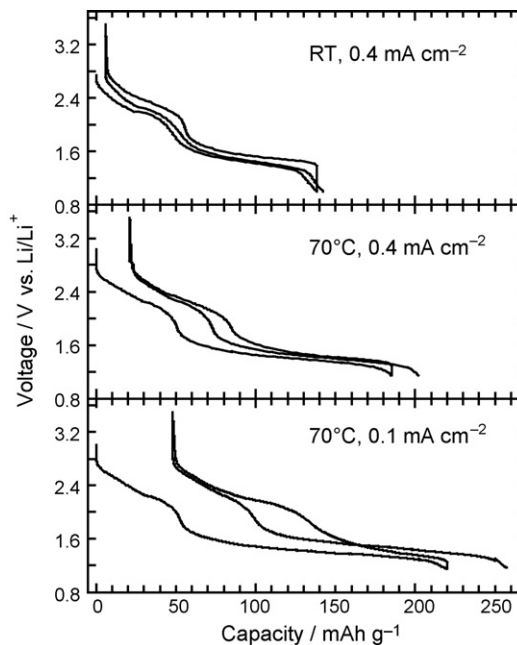


Fig. 8. Discharge/charge curves in initial first and half cycles of $\text{Li}_{1.78}[\text{Li}_{0.38}\text{Fe}_{0.63}\text{Ti}_{2.99}]\text{O}_8$ electrode at different operating temperatures and current density in electrolyte of 1 M LiPF_6 EC/DMC 1:2 (in volume). Voltage range: 1.0–3.5 V for RT and 1.15–3.5 V for 70 °C.

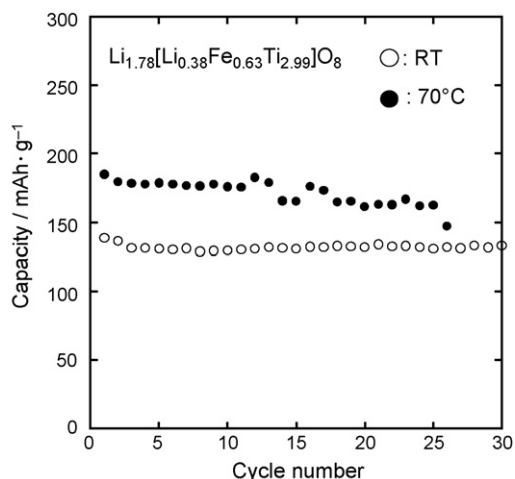


Fig. 9. Variation of specific discharge capacity with cycle number for $\text{Li}_{1.78}[\text{Li}_{0.38}\text{Fe}_{0.63}\text{Ti}_{2.99}]\text{O}_8$ electrode at RT and 70 °C in electrolyte of 1 M LiPF_6 EC/DMC 1:2 (in volume). Galvanostatic current density: 0.4 mA cm^{-2} ; voltage range: 1.0–3.5 V for RT and 1.15–3.5 V for 70 °C.

Fig. 8. It can be found that the elevated operating temperature also increased the discharge/charge capacity, e.g., from 138.2 mAh g^{-1} at RT to 185.6 mAh g^{-1} at 70 °C for the initial discharge. More importantly, the increased Fe content further improved the cycling performance of ramsdellite sample at 70 °C as shown in Fig. 9. The stabilization of Fe on $\text{Li}_2\text{Ti}_3\text{O}_7$ ramsdellite lattice framework maybe come from the smaller ion radius of Fe^{3+} than Ti^{4+} , Fe^{3+} (0.69 \AA) < Ti^{4+} (0.745 \AA) [16], which would be expected to enhance the attractive action between central cations and framework oxygen anions, and thus improve the stability of the ramsdellite structure to lithium ions intercalation/deintercalation at elevated temperatures. Here, it should be noted that the similar stabilization effect could be found in their preparing easiness. $\text{Li}_2\text{Ti}_3\text{O}_7$ ramsdellite and its Fe-doped variant were obtained at different firing temperatures for stable structures. Among them, the Fe-doped ramsdellite produced at a much decreased temperature of 950 than 1050 °C in $\text{Li}_2\text{Ti}_3\text{O}_7$, which are probably from the same stabilization effect of the Fe^{3+} ions with smaller radius than Ti^{4+} .

4. Conclusions

The high temperature electrochemical cell performances of $\text{Li}_2\text{Ti}_3\text{O}_7$ and its Fe-doped derivatives were studied. Pure $\text{Li}_2\text{Ti}_3\text{O}_7$ gave a high stable discharge/charge capacity of

160 mAh g^{-1} at 50 °C relative to 130 mAh g^{-1} at room temperature and a good cycleability. However, the cell performance was terribly deteriorated at 70 °C. XRD measurement revealed its structure degradation into a rocksalt-type cubic structure phase with lower crystallinity in this high temperature of 70 °C. The XRD results from the electrodes experienced different cycles at 40 °C showed that the structure degradation is gradually developed as the cell is cycled. Meanwhile, both Fe-doped $\text{Li}_2\text{Ti}_3\text{O}_7$ ramsdellite samples afforded improved insertion/extraction properties of the lithium ions, even at 70 °C. The improved high temperature performance is presumedly considered from the stabilization of the foreign iron metal ions with a smaller ion radius, Fe^{3+} (0.69 \AA) < Ti^{4+} (0.745 \AA), for ramsdellite structure. The Fe-doped $\text{Li}_2\text{Ti}_3\text{O}_7$ ramsdellite, especially one with a higher Fe content, is available as anode material for lithium ion batteries at elevated operating temperatures up to 70 °C.

References

- [1] W.C. Mackrodt, J. Solid State Chem. 142 (1999) 428.
- [2] T. Ohzuku, A. Ueda, N. Yamamoto, J. Electrochem. Soc. 142 (1995) 1431.
- [3] S. Schärer, W. Weppner, P. Schmid-Beurmann, J. Electrochem. Soc. 146 (1999) 857.
- [4] S. Garnier, C. Bohnke, O. Bohnke, J.L. Fourquet, Solid State Ionics 83 (1996) 323.
- [5] M.E. Arroyo y de Dompablo, E. Moran, A. Varez, G. Gareia-Ala varado, Mater. Res. Bull. 32 (1997) 993; R.K.B. Gover, J.R. Tolchard, H. Tukamoto, T. Murai, J.T.S. Irvine, J. Electrochem. Soc. 146 (1999) 4348.
- [6] M.A. Arillo, M.L. Lopez, E. Perez-Cappe, C. Pico, M.L. Veiga, Solid State Ionics 107 (1998) 307.
- [7] K.S. Yoo, N.W. Cho, Y.-J. Oh, Solid State Ionics 113–115 (1998) 43.
- [8] M.A. Arillo, M.L. Lopez, M.T. Fernandez, M.L. Veiga, C. Pico, J. Solid State Chem. 125 (1996) 211.
- [9] A.D. Robertson, L. Trevino, H. Tukamoto, J.T.S. Irvine, J. Power Sources 81–82 (1999) 352.
- [10] M.E. Arroyo y de Dompablo, A. Varez, F. Garcia-Alvarado, J. Solid State Chem. 153 (2000) 132.
- [11] L. Kavan, D. Fattakhova, P. Krtil, J. Electrochem. Soc. 146 (1999) 1375.
- [12] T. Ohzuku, K. Tatsumi, N. Matoba, K. Sawai, J. Electrochem. Soc. 147 (2000) 3592.
- [13] M. Yoshio, A. Kozawa, Lithium Ion Secondary Batteries—Materials and Application, Nikkan Kogyo Shinbun Sya, 2000.
- [14] G. Zhuang, P.N. Ross Jr., J. Power Sources 89 (2000) 143.
- [15] S. Ma, H. Noguchi, Electrochemistry (Denki Kagaku) 69 (7) (2001) 63.
- [16] Denki Kagaku Benran (Electrochemical Handbook), Version 4, Maruzen Inc., 1985, p. 24.